Lattice statistics in three dimensions: Solution of layered dimer and layered domain wall models

V. Popkov* and Doochul Kim
Department of Physics and Center for Theoretical Physics, Seoul National University, Seoul 151-742, Korea

H. Y. Huang and F. Y. Wu
Department of Physics and Center for Interdisciplinary Research in Complex Systems, Northeastern University, Boston, Massachusetts 02115

(Received 5 March 1997)

Analyses are given for two three-dimensional lattice systems: A system of close-packed dimers placed in layers of honeycomb lattices and a layered triangular-lattice interacting domain wall model, both with nontrivial interlayer interactions. We show that both models are equivalent to a five-vertex model on the square lattice with interlayer vertex-vertex interactions. Using the method of Bethe ansatz, a closed-form expression for the free energy is obtained and analyzed. We deduce the exact phase diagram and determine the nature of the phase transitions determined as a function of the strength of the interlayer interaction. [S1063-651X(97)07010-4]

PACS number(s): 05.50.+q

I. INTRODUCTION

An important milestone in the field of exact solutions of lattice-statistical systems is the solution of close-packed dimers on planar lattices obtained by Kasteleyn [1] and by Fisher [2]. However, there has since been very little progress in extending the dimer solution to higher dimensions. To be sure, Bhattacharjee *et al.* [3] have studied dimers on a certain three-dimensional (3D) lattice using numerical means, and two of us [4] have solved a vertex model in arbitrary d dimension, a solution which also solves a dimer problem in d dimension. In the latter case, however, the dimer model involves unphysical negative statistical weights.

In a recent Letter [5], hereafter referred to as I, three of us reported on the solution of a 3D dimer system as an instance of a more general class of soluble 3D lattice-statistical problem. In contradistinction with other exactly solved 3D systems [6,7] which invariably involve negative Boltzmann weights, the formulation reported in I, which generalizes other special cases reported elsewhere [8], marks the success of solving a 3D lattice-statistical model with strictly positive Boltzmann weights. In this paper we present details of this solution. In addition, we show also that our solution solves a layered domain wall model with interlayer interactions.

This paper is organized as follows. In Sec. II we define a layered dimer system with interlayer interactions and its equivalent layered five-vertex model. The description of an equivalent layered domain wall model is given in Sec. III. The free energy of the 3D system is analyzed in Sec. IV with the phase diagram obtained in Sec. V. The critical behavior is deduced in Sec. VI. Finally in Sec. VII we discuss the occurrence of infinite degeneracy of orders in the system.

II. A LAYERED DIMER SYSTEM AND THE EQUIVALENT FIVE-VERTEX MODEL

Consider a 3D lattice $\mathcal{L}$ consisting of K layers of honeycomb lattices stacked together as shown in Fig. 1. Each layer of $\mathcal{L}$ is a honeycomb dimer lattice in which dimers with weights u,v,w are placed in the three respective lattice directions. The dimers are close packed within each layer and interact with an interlayer interaction shown in Table I which gives, for example, the interaction energy $2h/3$, and hence a Boltzmann factor $e^{-2h/3}$, between a u dimer in the kth layer and a v dimer in the $(k+1)$th layer. This completes the description of our 3D dimer system. The interlayer coupling introduced here is admittedly artificial and we do not conjecture about possible physical applications. However, the merit of the model is that it is integrable, enabling one to study its properties exactly.

Since a perusal of Table I shows that the negation of h corresponds to the interchange of the layers k and $k+1$, we can without loss of generality take $h \geqslant 0$.

The honeycomb dimer system can be formulated as a

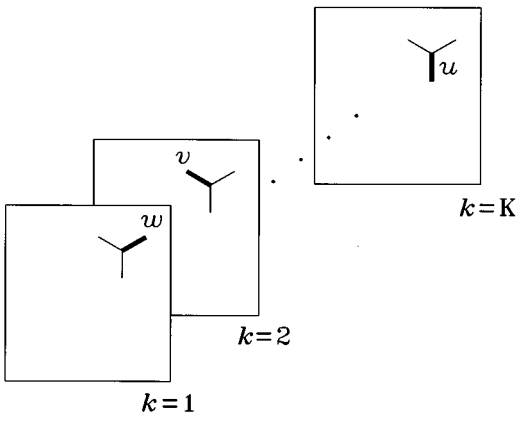

FIG. 1. A three-dimensional lattice model consisting of layers of honeycomb dimer lattices.

*Permanent address: Institute for Low Temperature Physics, Kharkov, Ukraine.

TABLE I. Interaction energy between two dimers incident at the same site of adjacent layers. The interaction is symmetric in u,v,w.

Layer $k\to k+1$	u	v	w
u	0	$2h/3$	$-2h/3$
v	$-2h/3$	0	$2h/3$
w	$2h/3$	$-2h/3$	0

five-vertex model on a square lattice [9]. This can be seen by drawing the honeycomb lattice in the form of a ''brick wall'' as shown in Fig. 2. The shrinking of each box containing two lattice points connected by a w edge into a point then converts the honeycomb lattice into a square lattice. By regarding the presence of a u or v dimer on the remaining honeycomb edges as being bonds, each dimer configuration is then mapped into a vertex configuration of a five-vertex model, and vice versa. The resulting five-vertex configurations and weights [9] are shown in Fig. 3.

Furthermore, the interlayer dimer interaction leads to an interlayer vertex interaction. It turns out that the interlayer vertex-vertex interaction corresponding to Table I is not unique. To deduce a useful interlayer vertex-vertex interaction we first modify Table I by replacing the uu and vv entries by $2\epsilon h$, where $\epsilon=+1(-1)$ for sites in sublattice A (B). Since two interacting uu or vv dimers are always parallel covering a pair of A and B sites, this replacement does not alter the overall interaction energy. A little algebra then shows that the dimer interaction of the modified Table I leads to the interlayer vertex interactions shown in Table II. Thus we have at hand a layered five-vertex model with interlayer interactions.

Let each square lattice be of size $M\times N$, with M sites in a column and N sites in a row. This corresponds to MNK dimers on $\mathcal{L}$. Label sites of the layers of square lattices by indices $\{m,j,k\}$, with $m=1,\ldots,M$, $j=1,\ldots,N$, and $k=1,\ldots,K$. Denote the vertex weight at site $\{m,j,k\}$ by W_{mjk}, and denote the interaction in Table II between vertices $\{m,j,k\}$ and $\{m,j,k+1\}$ by B_{mjk}. Then, it is our goal to evaluate the partition function

$$Z_{MNK}=\sum_{\text{config}}\prod_{k=1}^{K}\prod_{m=1}^{M}\prod_{j=1}^{N}(B_{mjk}W_{mjk}), \tag{1}$$

where the summation is taken over all dimer, or vertex, configurations, and the *per-dimer* free energy

$$f=K^{-1}\lim_{M,N\to\infty}(MN)^{-1}\ln Z_{MNK}. \tag{2}$$

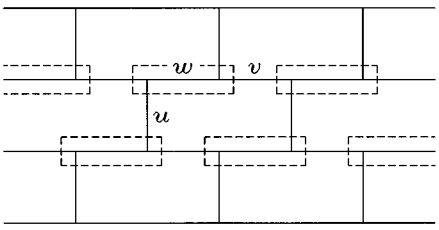

FIG. 2. The mapping of a honeycomb lattice onto a square lattice.

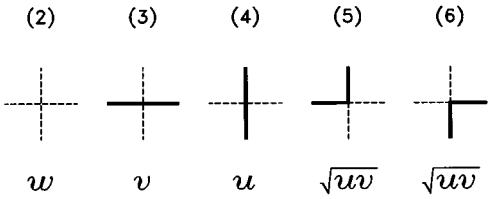

FIG. 3. Vertex configurations and weights of the five-vertex model.

For simplicity, we shall assume $K=3\times$ integers. We also assume periodic boundary conditions.

To write the interlayer vertex interactions of Table II in the form of B_{mjk}, we introduce variables $\alpha_{mjk}=\pm1$ and $\beta_{mjk}=\pm1$, respectively, for the horizontal and vertical edges within the kth layer and originating from the site $\{m,j,k\}$ in the direction of, say, decreasing $\{m,j\}$, such that $\alpha_{mjk}=+1(-1)$ corresponds to the edge having a bond (empty). It is then straightforward to verify that the vertex-vertex interactions in Table II can be written as

$$\varepsilon=-h(\alpha_j\widetilde{\beta}_j-\widetilde{\alpha}_{j+1}\beta'_j)-\frac{h}{3}(\alpha_j-\widetilde{\alpha}_{j+1})-\frac{h}{3}(\widetilde{\beta}_j-\beta'_j), \tag{3}$$

where we have, for convenience, suppressed the subscripts m and k by adopting the notation

$$\beta_{m+1,j,k}\to\beta'_j,\quad \beta_{m,j,k+1}\to\widetilde{\beta}_j, \tag{4}$$

and similarly for the α's. Now the second and third terms in Eq. (3) are cancelled upon introducing this interaction into the overall partition function (1). This leads to an effective Boltzmann factor

$$B_{mjk}=\exp[h(\alpha_j\widetilde{\beta}_j-\widetilde{\alpha}_{j+1}\beta'_j)], \tag{5}$$

which is to be used in Eq. (1).

III. A LAYERED DOMAIN WALL MODEL

In this section we show that the layered dimer and five-vertex models of the preceding sections also describe a layered domain wall model with interlayer interactions.

Consider a 3D lattice consisting of K layers of triangular lattices whose faces are elementary (up-pointing and down-pointing) triangles. Sites of the triangular lattices are occupied by Ising spins $\sigma=\pm$ with the constraint that, around each face of the lattice, there are precisely two spins of the

TABLE II. Interaction energy between two vertex configurations of adjacent layers. ω_i, $i=2,\ldots,6$ denotes the vertex of type i in Fig. 3.

Layer $k-k+1$	ω_2	ω_3	ω_4	ω_5	ω_6
ω_2	0	$-4h/3$	$4h/3$	0	0
ω_3	$4h/3$	0	$-4h/3$	$4h/3$	$-8h/3$
ω_4	$-4h/3$	$4h/3$	0	$-4h/3$	$8h/3$
ω_5	0	$8h/3$	$-8h/3$	0	0
ω_6	0	$-4h/3$	$4h/3$	0	0

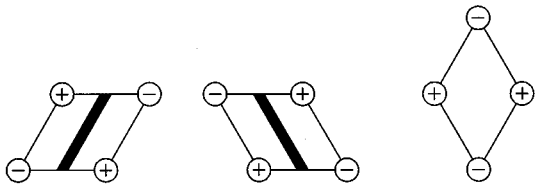

FIG. 4. The three possible orientations of a diamond. Strips are associated with diamonds oriented in two particular directions.

same sign and one spin of the opposite sign. The allowed spin configurations are those of the ground state of an isotropic antiferromagnetic Ising model. Furthermore, if one erases lattice edges connecting two spins of the same sign, one arrives at a diamond (or rhombus) covering of the triangular lattice. This can be interpreted as a dimer covering of the dual honeycomb lattice, by placing dimers connecting the two dual lattice points on the elongated diagonal of each rhombus. It is clear that the mapping between the spin configurations and the diamond and dimer coverings is two to one. Indeed, this mapping has been used to extract the solution of the honeycomb dimer lattice from the Ising ground state [10].

The spin configurations can also be viewed as representing domain wall configurations [10,11]. This mapping is most conveniently seen [11] from the associated diamond covering scheme. If one attaches strips to those diamonds oriented in two of the three possible directions as shown in Fig. 4, then the strips form continuous lines and propagate in a zigzag but generally vertical direction, which can be interpreted as representing domain walls (cf. Figs. 2 and 4 of [11] for a typical domain wall configuration). A spin configuration is thus mapped into a domain wall configuration Specifically, the triangular faces of the lattice can be in one of the six ''strip'' configurations shown in Fig. 5, and the domain wall model is defined by associating weights to the triangles as shown in Fig. 5.

Next we introduce interlayer domain wall interactions. Shift the $(k+1)$th layer by half lattice constant to the left with respect to the kth layer so that the up-pointing (down-pointing) triangles in the layer k will be adjacent to down-pointing (up-pointing) triangles in the layer $k+1$. Let two adjacent triangular faces in planes k and $k+1$ interact with an energy shown in Table III. Together with the triangle weights given in Fig. 5, this completely defines the layered domain wall problem. More precisely, the partition function for the domain wall problem is given by Eq. (1) now with the summation extending over all domain wall configurations, W_{mjk} representing the product of the triangle weights given

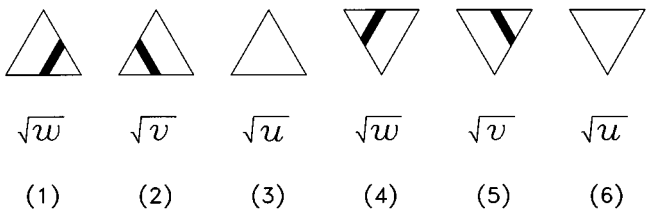

FIG. 5. The six strip configurations and the associated weights of a triangle.

TABLE III. Interaction energy between two strip triangles of adjacent layers. The triangle configurations are as numbered in Fig. 5.

Layer $k\rightarrow k+1$	1	2	3	4	5	6
1	0	0	0	0	$-2h$	0
2	0	0	0	$2h$	0	0
3	0	0	0	0	0	0
4	0	$-2h$	0	0	0	0
5	$2h$	0	0	0	0	0
6	0	0	0	0	0	0

in Fig. 5 and B_{mjk} the interlayer interaction given by Table III.

The mapping of a domain wall configuration to a five-vertex arrow configuration is given in [11], where the triangular lattice was deformed into a square lattice by tilting it clockwise, leading to a five-vertex model with $\omega_3=0$ (instead of $\omega_1=0$ as in Fig. 3). For the present paper, we deformed the triangular lattice by tilting it counterclockwise. Then, the vertex weights reduce exactly to those given in Fig. 3.

To obtain an explicit form for B_{mjk}, it is straightforward to verify that the interaction of Table III can be written as, in the language of the layered five-vertex model,

$$\varepsilon=-h(\alpha_j\tilde{\beta}'_j-\tilde{\alpha}_{j+1}\beta_j)+h(\alpha_j-\tilde{\alpha}_{j+1})-h(\tilde{\beta}'_j-\beta_j). \tag{6}$$

Again the second and third terms in Eq. (6) are cancelled in the overall partition function (1). But the effective interaction Boltzmann factor now assumes the form

$$B_{mjk}=\exp[h(\alpha_j\tilde{\beta}'_j-\tilde{\alpha}_{j+1}\beta_j)], \tag{7}$$

which differs slightly from Eq. (5) for the dimer problem. However, repeating precisely the same line of argument as in I, one can show that the interlayer interaction (7) leads to precisely the same free energy (9) and (8) given below. Thus the domain wall problem (with interlayer interactions of Table III) is completely equivalent to the dimer system (with interlayer interactions of Table I).

IV. THE FREE ENERGY

In the preceding sections we have established the complete equivalence of the layered dimer and domain wall problems, and their further equivalence with a layered five-vertex model. In this section we analyze the free energy of the layered 5-vertex problem. For simplicity we use the language of the dimer system [12].

It has been shown in I that the layers of five-vertex models with interlayer interaction (5) can be solved by applying a transfer matrix in the vertical direction and a global Bethe ansatz consisting of the usual Bethe ansatz within each layer. This leads to the following expression for the free energy:

$$f(u,v,w,h)=\max_{-1\leqslant y_k\leqslant 1} f(\{y_k\}), \tag{8}$$

where

$$f(\{y_k\})=\ln u+\frac{1}{K}\sum_{k=1}^{K}\frac{1}{\pi}\int_0^{\pi(1-y_k)/2}\times\ln\left|\frac{w}{u}+\frac{v}{u}e^{2h(y_{k+1}-y_{k-1})}e^{i\theta}\right|d\theta. \tag{9}$$

Here,

$$y_k=\frac{1}{N}\sum_{j=1}^{N}\beta_j=\frac{1}{N}\sum_{j=1}^{N}\beta_j'$$

is a quantity conserved from row to row (of vertical edges) in the kth layer square lattice. Specifically, we have $y_k=1-2n_k/N$, where n_k is the number of vacant edges in a row. Analysis leading to Eq. (9) has been given in I and will not be reproduced here.

It is clear that for large u, v, or w, the system is frozen with complete ordering of u, v, or w dimers in all layers, and hence the free energies

$$f_U=\ln u,\quad U\text{ phase},$$
$$f_V=\ln v,\quad V\text{ phase}, \tag{10}$$
$$f_W=\ln w,\quad W\text{ phase}.$$

These are frozen orderings which we refer to as the U, V, and W phases, respectively. For large h, it is readily seen from Table I that the energetically preferred state is the one in which each layer is occupied by one kind of dimer, u, v, or w, and that the layers are ordered in the sequence of $\{u,w,v,u,w,v,\ldots\}$. This ordered phase is referred to as the H phase with the free energy

$$f_H=\frac{1}{3}\ln(uvwe^{4h}),\quad H\text{ phase} \tag{11}$$

obtained from a perusal of Table I.

For any layer with $y_k=+1$ the corresponding integral in Eq. (9) vanishes, and for $y_k=-1$ the integral can be evaluated using the integration formula

$$\frac{1}{\pi}\int_0^{\pi}\ln|A+Be^{i\theta}|d\theta=\max\{\ln|A|,\ln|B|\}. \tag{12}$$

Therefore the free energy (9) can be explicitly evaluated if $y_k=\pm1$ for all k. Further discussion of this case will be given in Sec. VII.

We have carried out analytic as well as numerical analyses of the free energy (9) for fixed u,v,w,h, and it was found that the set $\{y_k\}$ which gives the extremum value in Eq. (8) always repeats in multiples of 3, namely, satisfying [13]

$$y_{k+3}=y_k.$$

The following extremum sets of $\{y_k\}$ are found.

(1) $\{y_1,y_2,y_3\}=\{1,1,1\}$: In this case we have all $y_k=1$, and hence from Eq. (9)

$$f=f_U,\quad U\text{ phase}. \tag{13}$$

This gives rise to the U phase.

(2) $\{y_1,y_2,y_3\}=\{-1,-1,-1\}$: In this case we have all $y_k=-1$, and hence from Eq. (9)

$$f=\ln u+\frac{1}{\pi}\int_0^{\pi}\ln\left|\frac{w}{u}+\frac{v}{u}e^{i\theta}\right|d\theta=\begin{cases}f_W, & w>v,\quad W\text{ phase}\\ f_V, & v>w,\quad V\text{ phase}.\end{cases} \tag{14}$$

This gives rise to the W and V phases.

(3) $\{y_1,y_2,y_3\}=\{1,-1,-1\}$: Substituting this sequence of y_k values into Eq. (9) and making use of Eq. (12) in the resulting expression, one obtains

$$f=\ln u+\frac{1}{6\pi}\int_{-\pi}^{\pi}\ln\left|\frac{w}{u}+\frac{v}{u}e^{2h}e^{i\theta}\right|d\theta+\frac{1}{6\pi}\int_{-\pi}^{\pi}\ln\left|\frac{w}{u}+\frac{v}{u}e^{-2h}e^{i\theta}\right|d\theta$$

$$=\begin{cases}\frac{1}{3}f_U+\frac{2}{3}f_W, & ve^{-4h}<ve^{4h}<w \quad (15)\\ \frac{1}{3}f_U+\frac{2}{3}f_V, & w<ve^{-4h}<ve^{4h} \quad (16)\\ f_H, & ve^{-4h}<w<ve^{4h},\quad H\text{ phase}. \quad (17)\end{cases}$$

Now the free energies (15) and (16) can be discarded since they are always smaller than the largest of $\{f_U,f_V,f_W\}$. Thus this set of $\{y_k\}$ leads to a frozen ordering for sufficiently large h as indicated in Eq. (17), which is the H phase.

(4) $\{y_1,y_2,y_3\}=\{y,y,y\}$: In this case all $y_k=y$, where y maximizes the free energy (9). Then, substituting $y_k=y$ into Eq. (9) and carrying out the maximization in Eq. (8) by a straightforward differentiation with respect to y, one obtains

$$f=f_Y(y_0)\equiv\ln u+\frac{1}{\pi}\int_0^{\pi(1-y_0)/2}\times\ln\left|\frac{w}{u}+\frac{v}{u}e^{i\theta}\right|d\theta,\quad Y\text{ phase}, \tag{18}$$

where the extremum y_0 is given by

$$\frac{\pi}{2}(1-y_0)=\cos^{-1}\left[\frac{u^2-w^2-v^2}{2wv}\right]. \tag{19}$$

This is a disorder phase which we refer to as the Y phase. Note that, despite its apparent asymmetric appearance, the free energy $f_Y(y)$ is actually symmetric in u,v,w. Note that, for large $v\sim w$, we have

$$\frac{\pi}{2}(1-y_0)=\pi-\theta_0, \tag{20}$$

where θ_0 is small and given by

$$\theta_0^2=[u^2-(w-v)^2]/wv. \tag{21}$$

(5) $\{y_1,y_2,y_3\}=\{y_1,-1,-1\}$: This is the H phase with the u layers replaced by layers with $y_k=y_1$, so that the layer ordering is $\{y_1,w,v,y_1,w,v,\ldots\}$. This is a partially ordered phase which we refer to as the I_u phase. Again, the substitution of these values of $\{y_k\}$ into Eq. (9) and a straightforward maximization yield, after using Eq. (12),

$$f=f_{I_u}(y_{10})=\begin{cases}\frac{1}{3}[2f_W+f_Y(y_{10})], & w>ve^{4h(1+y_{10})} \quad (22)\\ \frac{1}{3}[2f_V+f_Y(y_{10})], & w<ve^{-2h(1+y_{10})} \quad (23)\\ \frac{1}{3}[\ln(vwe^{2h(1+y_{10})})+f_Y(y_{10})], & ve^{-2h(1+y_{10})}<w<ve^{2h(1+y_{10})}, \quad I_u \text{ phase,} \quad (24)\end{cases}$$

where $f_Y(y_{10})$ is defined in Eq. (18), with the extremum y_{10} given by

$$\frac{\pi}{2}(1-y_{10})=\cos^{-1}\left[\frac{u^2e^{8h}-w^2-v^2}{2wv}\right]. \tag{25}$$

The free energies (22) and (23) are discarded since they are always less than the largest of $\{f_W,f_V,f_Y(y_{10})\}$, and we have $f_Y(y_{10})<f_Y(y_0)$ by definition. Therefore the free energy of the I_u phase is given by Eq. (24). Note that, for large $v\sim w$, we have

$$\frac{\pi}{2}(1-y_{10})=\pi-\theta_1, \tag{26}$$

where θ_1 is small and given by

$$\theta_1^2=[u^2e^{8h}-(w-v)^2]/wv. \tag{27}$$

(6) $\{y_1,y_2,y_3\}=\{1,y_2,-1\}$: This is the H phase with the w layers replaced by layers with $y_{k+1}=y_2$, so that the layer ordering is $\{u,y_2,v,u,y_2,v,\ldots\}$. We refer to this as the I_v phase. Due to the intrinsic symmetry of the interlayer interaction, the free energy of the I_w phase is the same as that of I_u, given in Eq. (24), with the cyclic permutation of $u\to w\to v\to u$. Alternately, one can substitute these $\{y_k\}$ values into Eq. (9) and carry out the maximization. It can be verified that this leads to

$$f=f_{I_w}(y_{20})=\frac{1}{3}\left[2f_U+f_V+\frac{1}{\pi}\int_0^{\pi(1-y_{20})/2}\times\ln\left|\frac{v}{u}+\frac{w}{u}e^{4h}e^{i\theta}\right|d\theta\right], \quad I_w \text{ phase,} \tag{28}$$

with

$$\frac{\pi}{2}(1-y_{20})=\cos^{-1}\left[\frac{u^2-w^2e^{8h}-v^2}{2wve^{4h}}\right]. \tag{29}$$

(7) $\{y_1,y_2,y_3\}=\{1,-1,y_3\}$: This is the H phase with the v layers replaced by layers with $y_{k+2}=y_3$, so that the layer ordering is $\{u,w,y_3,u,w,y_3,\ldots\}$. We refer to this as the I_v phase. Again, the free energy of the I_v phase can be written down by symmetry. Alternately, the substitution of these values of $\{y_k\}$ into Eqs. (9) and (8) yields

$$f=f_{I_v}(y_{30})=\frac{1}{3}\left[2f_U+f_W+\frac{1}{\pi}\int_0^{\pi(1-y_{30})/2}\times\ln\left|\frac{v}{u}e^{4h}+\frac{w}{u}e^{i\theta}\right|d\theta\right], \quad I_v \text{ phase,} \tag{30}$$

with

$$\frac{\pi}{2}(1-y_{30})=\cos^{-1}\left[\frac{u^2-w^2-v^2e^{8h}}{2wve^{4h}}\right]. \tag{31}$$

V. THE PHASE DIAGRAM

Since the phase diagram must reflect the $\{u,v,w\}$ symmetry of the interlayer interaction given in Table I, it is convenient to introduce coordinates

$$X=\ln(v/w), \quad Y=(\sqrt{3})^{-1}\ln(vw/u^2) \tag{32}$$

such that any interchange of the three variables u, v, and w corresponds to a 120° rotation in the $\{X,Y\}$ plane. The phase boundaries are then determined by equating the free energies of adjacent phases. The results are collected in Fig. 6.

The phase diagrams depend on the value of h and are different in different regimes.

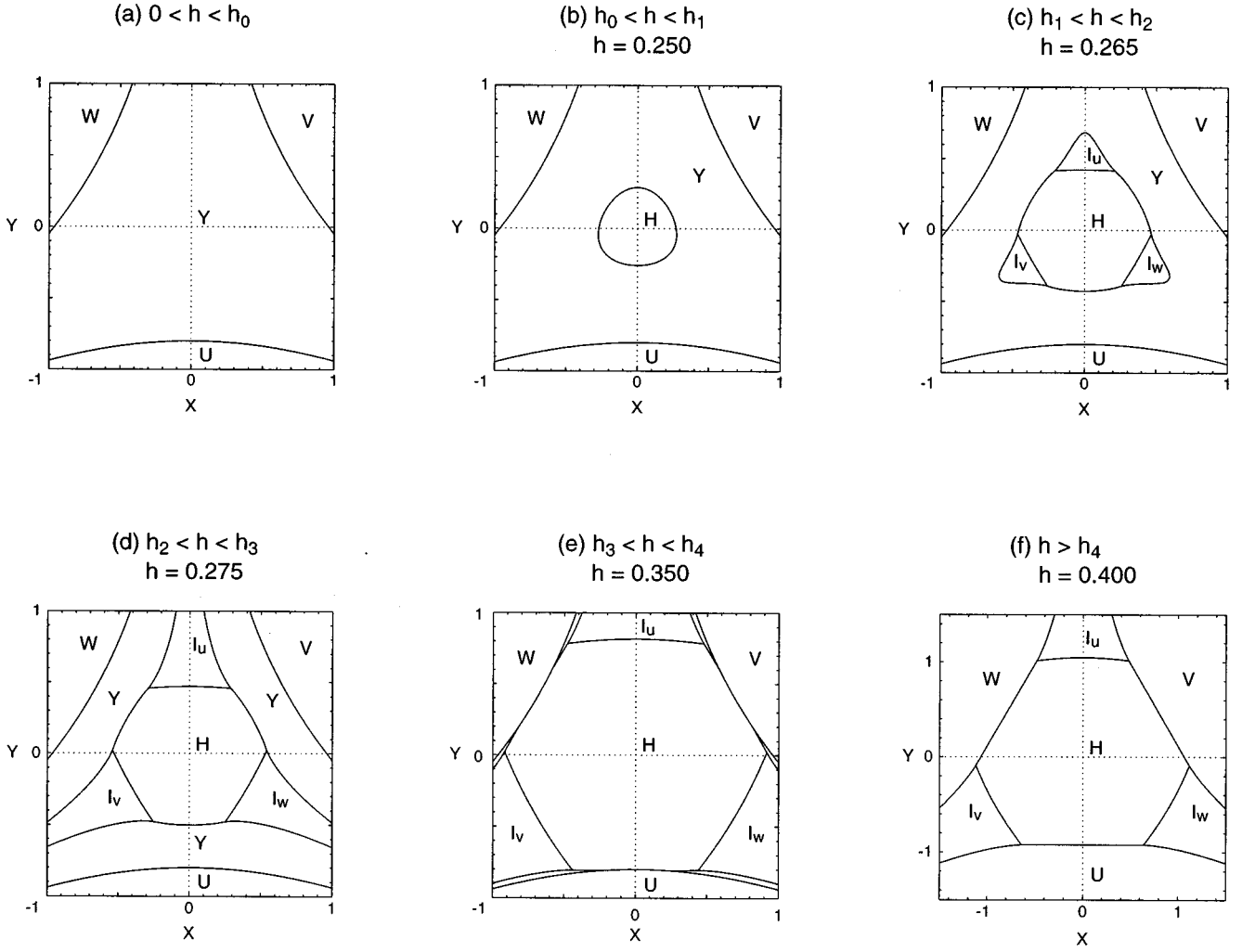

FIG. 6. Phase diagram of the 3D system.

(1) $h<h_0$: For small h the phase diagram is the same as that of the $h=0$ noninteracting 2D system, namely, the diagram shown in Fig. 6(a). The phase boundary between the $\{U,V,W\}$ phases and the Y phase, which stays the same in all regimes below, is obtained by setting $y_0=\pm 1$ in Eq. (19) where f_U, f_V, or f_W is equal to f_Y. These boundaries are

$$u=|v\pm w|. \tag{33}$$

In terms of the coordinates X and Y, $u=v+w$ and $u=|v-w|$ read, respectively,

$$Y=\frac{-2}{\sqrt{3}}\ln[2\cosh(X/2)], \quad Y=\frac{-2}{\sqrt{3}}\ln[2\sinh(|X|/2)].$$

(2) $h_0<h<h_1$: As h increases from zero, our numerical analyses indicate that the H phase appears when h reaches a certain value h_0. The resulting phase diagram is shown in Fig. 6(b). The phase boundary between the H and Y phases is given by $f_H=f_Y$, or, explicitly

$$\frac{1}{3}\ln(uvwe^{4h})=f_Y(y_0). \tag{34}$$

Thus h_0 is obtained from Eq. (34) by setting $u=v=w$ ($X=Y=0$) where the H phase first appears. This yields $\pi(1-y_0)/2=2\pi/3$ and

$$h_0=\frac{3}{8\pi}\int_0^{2\pi/3}\ln(2+2\cos\theta)d\theta=0.242\,299\,5\ldots. \tag{35}$$

(3) $h_1<h<h_2$: As h increases from h_0, the I_u, I_v,I_w phases appear when h reaches a certain value h_1. The resulting phase diagram is shown in Fig. 6(c). Now the I_u phase is the H phase with the u layers (with $y_k=1$) replaced by layers with $y_k=y_{01}$, the boundary between the two regimes is therefore given by $y_{10}=1$ or, explicitly using Eq. (25),

$$w+v=ue^{4h}. \tag{36}$$

The boundary between the I_u and the Y phases is $f_Y(y_0)=f_{I_u}(y_{10})$ or, explicitly,

$$\ln u+\frac{1}{\pi}\int_0^{\pi(1-y_0)/2}\ln\left|\frac{v}{u}+\frac{w}{u}e^{i\theta}\right|d\theta$$

$$=\frac{1}{3}\left[\ln(vwe^{2h(1+y_{10})})+\ln u+\frac{1}{\pi}\int_0^{\pi(1-y_{10})/2}\times\ln\left|\frac{v}{u}+\frac{w}{u}e^{i\theta}\right|d\theta\right]. \tag{37}$$

The boundaries of the I_v and I_w regimes can be written down similarly.

To compute the numerical value of h_1, we note that the I_u phase first appears at $v=w$ ($X=0$) when all three phases H, Y, and I_u coincide. Therefore h_1 is obtained by solving Eqs. (34) and (36) for v/u and h at $w=v$. This leads to the value

$$h_1=\frac{1}{4}\ln\left(\frac{2v}{u}\right)=0.255\,247\,9\ldots\ ,$$

where v/u is the solution of the equation

$$(1+y_0)\ln\frac{v}{u}+\frac{1}{6}(1+3y_0)\ln 2=\frac{1}{\pi}\int_0^{\pi(1-y_0)/2}\times\ln(1+\cos\theta)d\theta, \tag{38}$$

with

$$\frac{\pi}{2}(1-y_0)=\cos^{-1}\left(\frac{u^2}{2v^2}-1\right). \tag{39}$$

(4) $h_2<h<h_3$: As h increases from h_1, it was found that the regimes I_u, I_v, and I_w extends to infinite when h exceeds a certain value h_2. The phase diagram is shown in Fig. 6(d). The value of h_2 can be deduced from Eq. (37) in its large $w=v$ expansion. Setting $w=v$ in Eq. (37), introducing Eqs. (20) and (26) for large w, v, and equating the coefficients of $\ln(v/u)$ on both sides of the equation, one obtains

$$\frac{1}{\pi}(\pi-\theta_0)=\frac{1}{3}\left[2+\frac{1}{\pi}(\pi-\theta_1)\right], \tag{40}$$

or, simply, $\theta_0=\theta_1/3$. Now from Eqs. (21), (27), and $w=v$, we have the expressions $\theta_0=u/v$ and $\theta_1=(u/v)e^{4h}$. It follows that we have

$$h_2=(\ln 3)/4=0.274\,653\,0\ldots\ .$$

(5) $h_3<h<h_4$: As h increases from h_2, it was found that the boundary of the H phase bulges toward the U,V,W phases along the 30°, 150°, 270° lines, touching the U,V,W boundaries in these directions when h equals a certain value h_3. For $h>h_3$, the H phase borders directly with the U,V,W phases with respective boundaries

$$u^2=vwe^{4h},\ v^2=wue^{4h},\ w^2=uve^{4h}. \tag{41}$$

The size of these borders grows while the Y phase shrinks as h increases. The phase diagram in this regime is shown in Fig. 6(e). To determine h_3, we let the $\{H,Y\}$ phase boundary (34) touch the $\{Y,U\}$ phase boundary $u=w+v$ at $w=v$ (the 270° direction). Using Eq. (19) we have $y_0=1$, and it follows that Eq. (34) becomes

$$\frac{1}{3}[\ln(2v^3e^{4h})]=\ln(2v)+0$$

from which we find [14]

$$h_3=(\ln 2)/2=0.346\,573\,5\ldots\ .$$

(6) $h>h_4$: As h increases further from h_3, it was found that the Y phase disappears completely when h exceeds a certain value h_4. The phase diagram in this regime is shown in Fig. 6(f). To determine the numerical value of h_4, we note that the Y phase disappears when the boundary $v=w+u$ between the V and Y phases coincides with the boundary (37) between the I_u and Y phases at large w,v. Therefore we again expand Eq. (37) for large v,w but now subject to $v-w=u$. Introduce Eqs. (20) and (26) for the integration limits. But now from Eqs. (21) and (27) we have $\theta_0=0$, $\theta_1=\gamma u/\sqrt{wv}$, where

$$\gamma=\sqrt{e^{8h}-1}. \tag{42}$$

Substituting Eqs. (20) and (26) into Eq. (37) and making use of Eq. (12) and the relation (for $v>w$)

$$\frac{1}{\pi}\int_0^{\pi-\theta_1}\ln\left|\frac{v}{u}+\frac{w}{u}e^{i\theta}\right|d\theta=\ln\frac{v}{u}-\frac{1}{\pi}\int_0^{\theta_1}\ln\left|\frac{v}{u}-\frac{w}{u}e^{i\theta}\right|d\theta,$$

one obtains

$$\ln v=\frac{1}{3}\left[\ln(vwe^{4h\theta_1/\pi})+\ln v-\frac{1}{2\pi}\int_0^{\theta_1}\times\ln\left(\frac{v^2}{u^2}+\frac{w^2}{u^2}-\frac{2vw}{u^2}\cos\theta\right)d\theta\right]. \tag{43}$$

Since θ_1 is small, we can write $\cos\theta=1-\theta^2/2$ in the integrand, and the integral can be simplified by introducing the change of variable $y=\sqrt{wv}\,\theta/u$. Introducing $w=v-u$ and expanding Eq. (43) for large w,v using, for example, $\ln(vw)=2\ln v-u/v$, the leading terms of the order of $\ln v$ are cancelled. The next terms including the integral are of the order of $O(u/v)$. Setting the coefficient of these terms equal to zero, one obtains

$$4h\gamma=\pi+\frac{1}{2}\int_0^{\gamma}\ln(1+y^2)dy$$

$$=\pi+\frac{1}{2}\gamma\ln(1+\gamma^2)-\gamma+\tan^{-1}\gamma,$$

or, after using $1+\gamma^2=e^{8h}$,

$$\gamma-\tan^{-1}\gamma=\pi \tag{44}$$

whose solution gives h_4. Specifically, we find

$$h_4=\frac{1}{8}\ln(1+\gamma^2)=0.381\,695\,5\ldots\ .$$

Phase diagram for the domain wall model. Since the domain wall model with weights given in Fig. 5 and interlayer interactions of Table III is completely equivalent to the layered dimer system, the phase diagram of the domain wall model is the same as that of the dimer model. For example, the phase U corresponds to a phase with no domain walls, and the phase H corresponds to a sequence of triplets of layers with no domain walls, maximal density of domain walls consisting of elementary weights $\sqrt{w}$, and maximal density of domain walls of weights $\sqrt{v}$ (cf. Fig. 5).

VI. THE CRITICAL BEHAVIOR

In this section we determine the critical behavior at all phase boundaries. Since the free energies are given by different analytic expressions in different phase regimes, one generally expects the first derivatives of the free energy (with respect to a temperature T, say) be discontinuous. This then leads to first-order transitions. However, if the first derivatives of the free energies happen to vanish on both sides of the boundary, then one has continuous transition. Applying this analysis, we find all transitions to be of first order, except those between the $\{U,V,W\}$ and Y phases, and between the $\{I_u, I_v, I_w\}$ and H phases, which are found to be the same as the transition in the five-vertex model [9], namely, a continuous transition with a square-root singularity in the specific heat. This transition, first reported by one of us in 1967 [15], is now known as the Pokrovsky-Talapov type phase transition [16].

Regarding u, v, w, and e^h as Boltzmann factors, the ordered U, V, W, and H phases (with $y_k = \pm 1$) have constant free energies and hence zero first derivatives. Therefore, we focus on the boundaries of these frozen regimes.

We have seen that the transition between the U,V,W phases and the Y phase is the same as that of the 2D system, which is known [9] to be of second order. This fact can also be seen by expanding the free energy near y_0 as

$$f_Y(y) = f_Y(y_0) + (y-y_0) f_Y'(y_0) + \frac{1}{2!}(y-y_0)^2 f_Y''(y_0) + \frac{1}{3!}(y-y_0)^3 f_Y'''(y_0) + \cdots . \tag{45}$$

Using the expression of $f_Y(y)$ defined by Eq. (18), one sees that, indeed, the first derivative $f_Y(y_0)$, $y_0 = \pm 1$, vanishes identically on the boundary (33) which is precisely $f_Y'(y_0) = 0$. Furthermore, it is also seen that $f_Y''(y_0) \sim \sin[\pi(1-y_0)/2] = 0$. Therefore the extremum of $f_Y(y)$ (45) occurs at $y = y_{\text{extrm}}$ given by

$$y_{\text{extrm}} - y_0 = \pm \sqrt{\frac{2 f_Y'(y_0)}{-f_{lY}'''(y_0)}} \sim t^{1/2}, \tag{46}$$

where $t = |T - T_c|$, T_c being the critical temperature. Substituting this y_{extrm} into Eq. (45), one obtains

$$f_Y(y_{\text{extrm}}) = f_Y(y_0) \pm \frac{2}{3} f_Y'(y_0) \sqrt{\frac{2 f_Y'(y_0)}{-f_Y'''(y_0)}} = f_Y(y_0) + c(u,v,w,h) t^{3/2}. \tag{47}$$

This leads to a square-root singularity in the specific heat, which is a characteristic of the Pokrovsky-Talapov phase transition. The key element leading to this result is the fact that the boundary of the frozen phases is given precisely by $f_Y'(y_0) = 0$, rendering the first derivative of the free energy to vanish at the boundary.

Applying the same analysis to the H and I_u phases, the boundary is again given by $f_{I_u}'(y_{10}) = 0$. Furthermore, it is also seen that $f_{I_u}''(y_{10}) = 0$ identically. It follows that the analysis can be carried through exactly as given in the above, and one concludes

$$f_{I_u}(y_{\text{extrm}}) = f(y_{10}) + c_1(u,v,w,h) t^{3/2}. \tag{48}$$

This gives rise again to a square-root singularity in the specific heat. The consideration of the I_v, I_w, and the H boundaries can be done similarly.

VII. DEGENERACY OF ORDERED STATES

We discuss in this section the degeneracy of ordered states. Particularly, we show that the system has a nonzero per-layer entropy on the boundaries between H and U,V,W phases.

We first establish the occurrence of a degeneracy from an energy consideration. For this purpose it is sufficient to show that this is the case along the $\{H,V\}$ boundary (41), namely,

$$e^{4h} = v^2/wu. \tag{49}$$

We already know that, along the boundary (49), the following layer orderings of the H and V phase are degenerate,

$$\ldots 222222222 \ldots$$

$$\ldots (132)(132)(132) \ldots . \tag{50}$$

Here, for convenience, we have used the notations $\{1,2,3\}$ for $\{u,v,w\}$. Generally, when $y_k = \pm 1$, each layer contains dimers of only one kind, u, v, or w. Let α_i, $i = 1,2,3$ denote the numbers of u, v, and w layers, respectively, as a fraction of K, and α_{12} the fraction of adjacent pair of u,v layers, etc. Then, perusal of Table I shows that this leads to the per-site free energy

$$f = \frac{1}{2}(\alpha_1 \ln u + \alpha_2 \ln v + \alpha_3 \ln w) + \frac{2h}{3}(\alpha_{13} + \alpha_{32} + \alpha_{21} - \alpha_{12} - \alpha_{23} - \alpha_{31}). \tag{51}$$

Here, the α's satisfy the conservation rules $\alpha_1 + \alpha_2 + \alpha_3 = 1$, $\Sigma_j \alpha_{ij} = \alpha_i$.

Consider the following ordering:

$$\ldots 2(1)3222(1)322222(1)32 \ldots , \tag{52}$$

characterized by single u layers separating strings of layers of the type $wvvvvv \ldots$ where there is at least one v layer in each string. It is readily seen from Eq. (52) that we have

$$\alpha_{12}=\alpha_{23}=\alpha_{31}=0,$$

$$\alpha_{21}=\alpha_{32}=\alpha_{13}=\alpha_1=\alpha_3\equiv\alpha,\quad \alpha_2=1-2\alpha. \tag{53}$$

It is then a simple matter to substitute Eqs. (49), (53) into Eq. (51), obtaining $f=f_V$. Thus, any layer ordering having the structure of Eq. (52) is degenerate to f_V on the $\{V,H\}$ boundary. Obviously, the number of such structures is infinite as $K\to\infty$. Note that Eq. (50) is a special case of Eq. (52). This degeneracy has been confirmed in our numerical analysis of Eq. (9).

Generally if $y_k=\pm 1$ for all layers, the free energy (9) can be explicitly evaluated for any ordering. Let $p_{\sigma,\sigma'}$, $\sigma=\pm$, denote the fraction of layers with $y_k=-1$ such that $\{y_{k-1},y_k,y_{k+1}\}=\{\sigma,-,\sigma'\}$, where for brevity we denote ± 1 by $\pm$. Consider, for example, the domain $v<w$. A straightforward evaluation of Eq. (9) leads to the expression

$$f=\begin{cases}\alpha_+ \ln u+\alpha_- \ln w, & ve^{-4h}<ve^{4h}<w\\ \alpha_+ \ln u+(p_{++}+p_{-+}+p_{--})\ln v+p_{+-} \ln w+4hp_{-+}, & ve^{-4h}<w<ve^{4h},\quad H \text{ phase.}\end{cases} \tag{54}$$

The first line can be discarded since it is always smaller than the larger of $\ln u$ and $\ln w$. A degeneracy of states now occurs if the second line coincides with the free energy of any phase. In the case of the ordering (52), for example, it is translated to

$$\cdots-(+)----(+)-------(+)--\cdots .$$

Now since each $+$ layer is associated with precisely one $+-$ and one $-+$ neighbors, we have $\alpha_+=p_{+-}=p_{-+}$. The substitution of this relation and Eq. (49) into Eq. (54) now leads to $f=f_V$ in agreement with the energy consideration. The degenerate states on the $\{H,U\}$ and $\{H,W\}$ boundaries can be obtained by cyclic permutations of u,v,w.

The entropy of the ordered state (52) can be computed. We note that the main feature of Eq. (52) is that layers v are followed by either u or v layers, and u layers are followed by only w layers, and w layers by v. Then the degeneracy S of the sequence (52) is given by the trace of a transfer matrix as

$$S=\mathrm{Tr}(T^K)=\lambda_1^K+\lambda_2^K+\lambda_3^K\sim\lambda_1^K, \tag{55}$$

where

$$T=\begin{pmatrix}0&0&1\\1&0&1\\0&1&0\end{pmatrix}, \tag{56}$$

and λ_j's are the eigenvalues of T with $\lambda_1>|\lambda_j|$, $j=2,3$. We find

$$\lambda_1=\frac{1}{3}\left[1+\left(\frac{29}{2}+\frac{3\sqrt{93}}{2}\right)^{1/3}+\left(\frac{29}{2}-\frac{3\sqrt{93}}{2}\right)^{1/3}\right]$$
$$\sim 1.465\,57\ldots .$$

VIII. SUMMARY

We have considered a three-dimensional layered dimer system with interlayer interactions and its equivalent layered domain wall model, and analyzed its exact solution. It is found that the phase diagram, shown in Fig. 6, depends crucially on the strength of the interlayer interactions. There exist ordered U,V,W,H phases corresponding to, respectively, large dimer weights u,v,w and large interlayer interactions h. In addition, there also exist a disorder phase Y and partially ordered phases I_u,I_v,I_w. The phase boundaries are determined by equating the free energies of adjacent regimes. Particularly, the boundary between the U,V,W phases and the Y phase assume the simple form (33), between the H and Y phases the form (34), and between the H and I_u phases the form (36). All transitions are found to be of first order, except the transitions between the U,V,W phases and the Y phase, and the transitions between the I_u, I_v, I_w, and H phases, which are of second order with a square root singularity in the specific heat.

ACKNOWLEDGMENTS

Work by F.Y.W. and H.Y.H. has been supported in part by National Science Foundation Grants No. DMR-9313648 and No. 9614170, work by V.P. has been supported in part by INTAS Grants No. 93-1324 and No. 93-0633, and V.P. and D.K. by the Korea Science and Engineering Foundation through the SRC program.

[1] P. W. Kasteleyn, Physica (Amsterdam) **27**, 1209 (1961).
[2] M. E. Fisher, Phys. Rev. **124**, 1664 (1961).
[3] S. M. Bhattacharjee, J. F. Nagle, D. A. Huse, and M. E. Fisher, J. Stat. Phys. **32**, 381 (1983).
[4] F. Y. Wu and H. Y. Huang, Lett. Math. Phys. **29**, 205 (1993).
[5] H. Y. Huang, V. Popkov, and F. Y. Wu, Phys. Rev. Lett. **78**, 409 (1997).
[6] R. J. Baxter, Commun. Math. Phys. **88**, 185 (1983).
[7] V. V. Bazhanov and R. J. Baxter, J. Stat. Phys. **69**, 453 (1992).
[8] V. Popkov and B. Nienhuis, J. Phys. A **30**, 99 (1997); A. E.

Borovick, S. I. Kulinich, V. Yu. Popkov, and Yu. M. Strzhemechny, Int. J. Mod. Phys. B **10**, 443 (1996).
[9] F. Y. Wu, Phys. Rev. **168**, 539 (1968).
[10] H. Blöte and H. Hirhost, J. Phys. A **15**, L631 (1982).
[11] J. D. Noh and D. Kim, Phys. Rev. E **49**, 1943 (1994).
[12] H. Y. Huang, F. Y. Wu, H. Kunz, and D. Kim, Physica A **228**, 1 (1996).
[13] Except on the boundaries between the H phase and the U,V,W phases other layer orderings also set in. The occurrence of this degeneracy is discussed in Sec. VII.
[14] The occurrence of $h_3=(\ln 2)/2$ was not discussed in [5].
[15] F. Y. Wu, Phys. Rev. Lett. **18**, 605 (1967).
[16] V. L. Pokrovsky and A. L. Talapov, Phys. Rev. Lett. **42**, 65 (1979).